

# Organic light-emitting-diode-based plasmonic dark-field microscopy

Feifei Wei,<sup>1</sup> Yin Wan O,<sup>2</sup> Guixin Li,<sup>2</sup> Kok Wai Cheah,<sup>2</sup> and Zhaowei Liu<sup>1,\*</sup>

<sup>1</sup>Department of Electrical and Computer Engineering, University of California, San Diego, 9500 Gilman Drive, La Jolla, California 92093-0407, USA

<sup>2</sup>Department of Physics, Hong Kong Baptist University, 224 Waterloo Road, Kowloon Tong, Hong Kong, China

\*Corresponding author: zhaowei@ece.ucsd.edu

Received September 6, 2012; accepted September 13, 2012;  
posted September 17, 2012 (Doc. ID 175690); published October 16, 2012

We propose and demonstrate a compact, alignment-free dark-field microscopy technique, termed as organic light-emitting-diode-based plasmonic dark-field microscopy. Experimental results show that it is capable of forming dark-field images of the specimens utilizing a highly integrated chip-scale plasmonic condenser. This technique has high  $z$  resolution and high imaging contrast and is suitable for the dynamics study near the contact regions of living cells and the substrate. © 2012 Optical Society of America

OCIS codes: 240.6680, 130.3120.

Invented several hundred years ago, the optical microscope is still an irreplaceable tool for life science research today, because light is undoubtedly the best way to examine living cells noninvasively. As a special optical imaging technique, dark-field (DF) microscopy is a spectacular method to form high-contrast images of unstained transparent specimens. In order to form a bright specimen image on a dark background, oblique rays from every azimuth are allowed to strike the samples, but only light scattered from the specimens is collected by the objective, as is shown in Fig. 1(a) in a transmission mode. A bulky condenser with an opaque light stop in the middle is used to guide the illumination light and needs to be aligned precisely with a detection objective. In reflection DF microscopy, this process is fulfilled by a specially designed DF objective combined with a reflection cube. In both cases, the numerical aperture (NA) of imaging objectives used in a DF microscope has to be smaller than that of the illumination optics, which in return hampers the resolution.

To further utilize the imaging capability of high NA objectives, NA of 1.2–1.4 DF condensers such as paraboloid or cardioid condensers have been developed [1]. These condensers can greatly improve the imaging resolution, but they require special design and are sensitive to alignment [1,2]. Although conventional DF microscopy has excellent imaging capability, it either requires bulky condenser optics and precise alignment or special as well as expensive DF objectives. To circumvent the limitations of conventional DF microscopy, several surface plasmon (SP)-related techniques, such as fluorescent-dye-based plasmonic dark-field (PDF) microscopy [3], prism- or solid immersion lens (SIL)-based dark-field surface plasmon microscopy [4,5], and surface-wave-enabled dark-field aperture (SWEDA) [6], have been proposed and demonstrated recently. Although these techniques have many advantages compared to conventional DF microscopy, they also have limitations. For example, they require external light sources to either excite the SP field or project the image of the object to the SWEDA [3–6], which reduces the compactness of the systems. Also, both fluorescent-dye-based PDF microscopy and SWEDA only work at a narrow wavelength range, limited

either by the emission wavelength of the fluorescent dye or the optimized SWEDA structure [3,6].

In order to improve the overall performance and further compactify a PDF microscope, we propose an organic light-emitting diode (OLED)-based PDF microscopy. This technique integrates a plasmonic structure with an OLED to serve as an active plasmonic condenser (PC), shown in Fig. 1(b). Such integration not only eliminates the need for an external illumination light source but also significantly reduces the physical size of the light condenser. Similar to fluorescent-dye-based PDF microscopy [3], SP is used as the illumination source in this technique. It can be excited by the light-emitting molecules in the OLED through a near-field coupling mechanism. The evanescent field property of the SP wave assures a perfectly dark background for far-field detection, while the objects within the SP field region act as couplers to convert partial SP energy into propagating light [7]. Therefore, a high-contrast dark-field image of the specimen is formed if the propagating light is collected by conventional objectives. Because SP waves exponentially decay away from the metal surface, this technique possesses extremely high resolution and sensitivity along the  $z$  direction and is suitable for studying the dynamics of molecules and proteins that occur in the vicinity of the cell substrate interface.

The OLED-based PC in our experiment is composed of a layer of aluminum (Al) film deposited on top of an

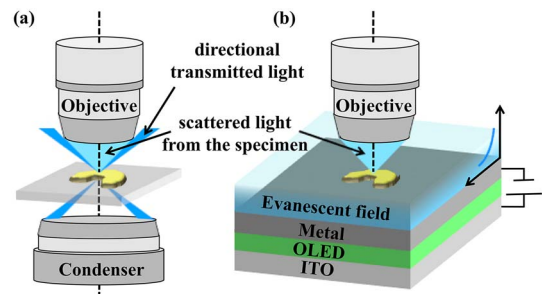


Fig. 1. (Color online) Schematic configuration of (a) conventional transmission mode DF microscope and (b) OLED-based PDF microscopy system.

OLED. Figures 2(a) and 2(b) illustrate the schematic configurations of the device in top view and cross-sectional view, respectively. The device was fabricated in a standard coater under the base vacuum of about  $10^{-6}$  Torr. 60 nm 2-TNATA film (4, 4', 4''-tris-[N-(2-naphthyl)-N-phenylamino]triphenylamine), 10 nm nondoped NPB film (N, N'-bis-(1-naphthyl)-N, N'-diphenyl, 1, 1'-biphenyl-4, 4'-diamine), 20 nm Alq<sub>3</sub> film (tris(8-quinolinolato)aluminium), and 1 nm LiF/60 nm Al film are used for hole injection, hole transport, electron transport, and electron injection layer, respectively [8–10]. When appropriate bias voltage is applied, the OLED emits white light from the indium tin oxide (ITO) side, as shown in Fig. 2(c). Figure 2(d) is a normalized electric luminance spectrum at 20 mA/cm<sup>2</sup> measured by a PR650 spectrophotometer with a DC source controlled by a connecting computer. The 60 nm Al film serves not only as the electrode for the OLED but also the SP supporting medium, where SP can be excited through near-field coupling with the organic light-emitting molecules in the blue and yellow emission layers. Therefore, there is no visible light emission from the Al side, as the SP waves are evanescent field. The choice of white light OLED enables a broadband detection across the whole visible spectrum. Note that a thin passivation layer (40 nm NPB) was also deposited on top of the metal film to keep the organic molecules from oxygen and water vapor to reduce their damage.

To demonstrate the imaging capability of the OLED-based PC, we fabricated a single layer of two-dimensional hexagonally close-packed lattice of the polystyrene beads (diameter 2  $\mu$ m) on top of the 40 nm NPB layer using a self-assemble method. Since the illumination SP waves exist only at the metal surface, no alignment between the PC and the detection objective is needed, as opposed to the case of conventional transmission DF microscopy. The scattered white light from the polystyrene particles was collected by a standard optical microscope objective (LD EC Epiplan-NEOFLUAR, 50 $\times$ , NA = 0.55) and then

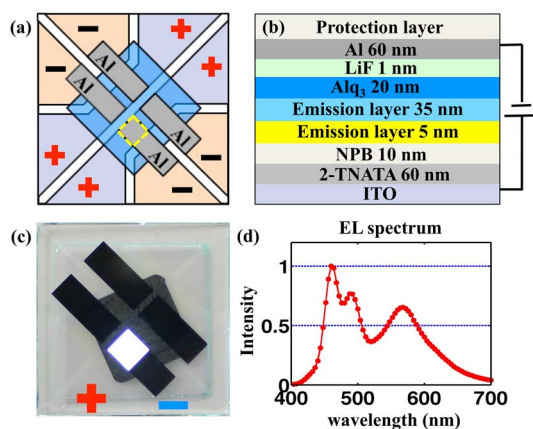


Fig. 2. (Color online) Schematic configurations of the device in (a) top view and (b) cross-sectional view. The purple area (labeled with “+”), brown area (labeled with “-”), and blue area are anode, cathode, and organic films (from 2-TNATA to Alq<sub>3</sub>), respectively. The overlap region is the light-emitting area, indicated by the (yellow) dashed square. (c) Photo of the OLED taken from the ITO side with 6 V DC voltage applied between the electrodes and (d) electric luminescence spectrum of the OLED at 20 mA/cm<sup>2</sup>.

captured by an Andor camera (iXonEM 897), shown in Figs. 3(a) and 3(b). The images express a bright signal at the region between the particles and a dim signal in the middle of the particles. The area with no presence of particles expresses as a dark background. Considering the refractive indices for polystyrene particle and air are 1.5 and 1, respectively, a bright scattering signal is obtained from the refractive index discontinuous region, which is the edges of the beads. This confirms that the image acquired is indeed a dark-field image, which is also consistent with results obtained by fluorescent-dye-based PDF microscopy demonstrated before [3]. Therefore, OLED-based PDF microscopy is capable of forming high-contrast images of objects lying close to the metal film with a highly integrated active PC without any additional light sources. We also performed an interpolation, noise reduction, and deconvolution process that has been widely applied to conventional microscopy imaging techniques, and the results are presented in Figs. 3(c) and 3(d), respectively. The signal-to-noise (S/N) ratio as well as overall image quality shows visible improvement.

Since the high-contrast imaging capability of the OLED-based PC comes from the evanescent nature of the SPs, the resolution along the direction perpendicular to the metal film as well as the S/N ratio strongly depend on the decay property of the SPs. Due to its short decay length, unwanted scattering from objects far from the interface can be avoided, and only objects within close vicinity to the plasmonic structure are imaged. Further increasing the *z* resolution and the S/N ratio can be realized by engineering the SP decay properties. Using carefully designed plasmonic structures suggested in the literature [11], the SP field with decay length much shorter than that created by other techniques such as total internal reflection can be achieved.

Besides the SP decay length, S/N ratio can also be influenced by other factors such as the coupling efficiency to SP and the surface roughness of the films. The coupling between the organic light-emitting molecules

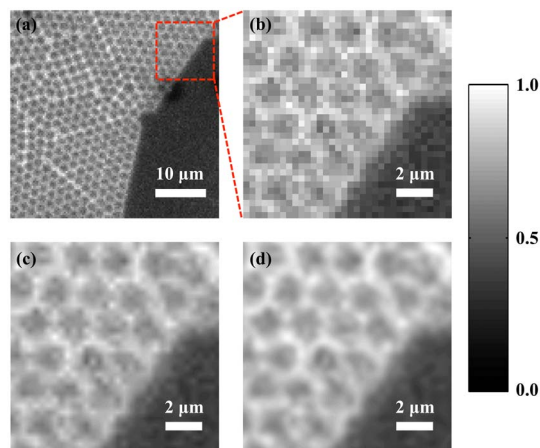


Fig. 3. (Color online) (a) Image obtained by OLED-based PDF microscopy, (b) magnified image of chosen area in (a), (c) interpolation of (b), and (d) noise reduction and deconvolution of (c). The objects are self-assembled polystyrene beads (diameter  $\sim$ 2  $\mu$ m). The observed image contrast (signal/background) enhancement is approximately 9 dB compared with bright field measurement.

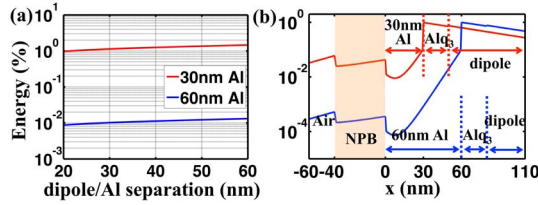


Fig. 4. (Color online) (a) Energy coupled to evanescent field at NPB/air interface for isotropically oriented dipole with emission wavelength at 460 nm, and (b) total E field intensity profile (log scale) with contribution from both SP modes supported by 30 nm Al (red [upper] curve) and 60 nm Al (blue [lower] curve), respectively.

and the plasmonic structure can be calculated by modeling the device as isotropically orientated dipoles in the vicinity of a metallic structure [12–14]. As is known, there are two plasmonic modes existing in OLED/Al/protection layer-air structure. The mode with a large wave vector is excited by the evanescent field of OLED light-emitting dipoles, while the other one with a relative small wave vector can be excited either by the propagating light or evanescent field generated by the light-emitting dipoles, depending on its wave vector and the refractive indices of the dielectric layers inside OLED. After considering the contribution from both SP modes, about 0.01% of the energy is coupled to the field on the air side [Fig. 4(a) blue {lower} curve], and it can be increased by 100 times by reducing Al thickness to 30 nm [Fig. 4(a) red {upper} curve] to decrease the attenuation of the large  $k$  vector mode through metal film as well as increase the coupling efficiency of the relative small  $k$  vector mode, as indicated by the total intensity distribution in Fig. 4(b). Besides decreasing the metal film thickness, the efficiency can be further increased by optimizing dipole/metal distance and protection layer thickness as well as refractive index, replacing Al to less lossy metal such as Ag, etc. The remaining energy is either coupled to lossy waves, emitted from the ITO side of the OLED, or transmitted through 60 nm Al film. Besides the direct transmitted light through metal film, photons rising from the scattering of the SP by surface roughness (2 nm rms for our device) also contribute to the background. The S/N ratio for the prototype device is about 2.4 and can be enhanced by increasing the coupling efficiency to SP, reducing film surface roughness by better deposition technique, etc. The dark circular defect at the top right of Fig. 3(a) is caused by the damage of the organic light-emitting molecules due to oxygen and water vapor and can be avoided by an improved passivation method [15–17]. We want to emphasize that the image acquisition time in the current demonstration can be reduced for real-time microscopy applications by increasing the coupling efficiency to SP, increasing OLED power, or using higher electronic gain for an imaging CCD detector.

As our experimental results show, OLED-based PDF microscopy is a highly compact, alignment-free approach to achieve high-contrast imaging of objects close to the interface. Since its dark-field imaging capability is enabled by evanescent field illumination instead of oblique ray illumination, OLED-based PDF microscopy doesn't

set any constraint on the NA of the detection objectives. Therefore, the capability of high NA objectives can be fully utilized to form high-resolution DF images. Moreover, since the principles of OLED-based PDF microscopy are similar to fluorescent-dye-based PDF microscopy, it shares the same advantages, such as large field of view, potential applications to fluorescent microscopy, etc. [3,18,19]. By integrating plasmonic structure with the white light OLED, white light OLED-based PC is more compact and can work across the whole visible spectrum compared with fluorescent-dye-based PC, prism- or SIL-based dark-field surface plasmon microscopy, and SWEDA [3–6]. Through an appropriate specimen-removing process, the device can be recycled for multiple measurements. The PC can also be further integrated with other lab-on-a-chip structures, such as microfluid channels, etc., to accomplish dark-field high-contrast imaging on a multifunction chip. It may have potential applications in fields such as bioimaging, sensing, and point-of-care diagnostics.

This work is partially supported by the start-up fund of the University of California at San Diego and the National science foundation, electrical, communication and cyber systems (NSF-ECCS) under Grant No. 0969405.

## References

1. D. B. Murphy, *Fundamentals of Light Microscopy and Electronic Imaging* (Wiley-Liss, 2001).
2. S. M. Prince and W. G. McGuigan, Proc. SPIE **6676**, 66760K (2007).
3. H. Hu, C. Ma, and Z. Liu, Appl. Phys. Lett. **96**, 113107 (2010).
4. J. Zhang, M. C. Pitter, S. Liu, C. See, and M. G. Somekh, Appl. Opt. **45**, 7977 (2006).
5. S. Balci, E. Karademir, C. Kocabas, and A. Aydinli, Opt. Lett. **36**, 3401 (2011).
6. G. Zheng, X. Cui, and C. Yang, Proc. Natl. Acad. Sci. USA **107**, 9043 (2010).
7. H. Raether, *Surface Plasmons on Smooth and Rough Surfaces and on Gratings* (Springer-Verlag 1988).
8. M. F. Lin, L. Wang, W. K. Wong, K. W. Cheah, H. L. Tam, M. T. Lee, and C. H. Chen, Appl. Phys. Lett. **89**, 121913 (2006).
9. M. F. Lin, L. Wang, W. K. Wong, K. W. Cheah, H. L. Tam, M. T. Lee, M. H. Ho, and C. H. Chen, Appl. Phys. Lett. **91**, 073517 (2007).
10. C. L. Ho, M. F. Lin, W. Y. Wong, W. K. Wong, and C. H. Chen, Appl. Phys. Lett. **92**, 083301 (2008).
11. Y. Xiong, Z. Liu, C. Sun, and X. Zhang, Nano Lett. **7**, 3360 (2007).
12. G. W. Ford and W. H. Weber, Phys. Rep. **113**, 195 (1984).
13. W. L. Barnes, J. Mod. Opt. **45**, 661 (1998).
14. P. Andrew and W. L. Barnes, Science **306**, 1002 (2004).
15. S. K. Park, J. Oh, C. Hwang, J. Lee, Y. S. Yang, and H. Y. Chu, Electrochem. Solid-State Lett. **8**, H21 (2005).
16. J. Park, H. Chae, H. K. Chung, and S. I. Lee, Semicond. Sci. Technol. **26**, 034001 (2011).
17. T. Riedl, J. Meyer, H. Schmidt, T. Winkler, and W. Kowalsky, "Thin film encapsulation of top-emitting OLEDs using atomic layer deposition," presented at Solid-State and Organic Lighting, Karlsruhe, Germany, June 21–24, 2010, p. SOWB5.
18. D. Axelrod, Traffic **2**, 764 (2001).
19. D. Axelrod, Methods Cell Biol. **89**, 169 (2008).